nature neuroscience

Synaptic basis for intense thalamocortical activation of feedforward inhibitory cells in neocortex

Scott J Cruikshank[1], Timothy J Lewis[2] & Barry W Connors[1]

The thalamus provides fundamental input to the neocortex. This input activates inhibitory interneurons more strongly than excitatory neurons, triggering powerful feedforward inhibition. We studied the mechanisms of this selective neuronal activation using a mouse somatosensory thalamocortical preparation. Notably, the greater responsiveness of inhibitory interneurons was not caused by their distinctive intrinsic properties but was instead produced by synaptic mechanisms. Axons from the thalamus made stronger and more frequent excitatory connections onto inhibitory interneurons than onto excitatory cells. Furthermore, circuit dynamics allowed feedforward inhibition to suppress responses in excitatory cells more effectively than in interneurons. Thalamocortical excitatory currents rose quickly in interneurons, allowing them to fire action potentials before significant feedforward inhibition emerged. In contrast, thalamocortical excitatory currents rose slowly in excitatory cells, overlapping with feedforward inhibitory currents that suppress action potentials. These results demonstrate the importance of selective synaptic targeting and precise timing in the initial stages of neocortical processing.

The neocortex, which comprises the majority of the mammalian brain, is critical for sensation, perception, goal-directed behavior and cognition[1]. It contains two general classes of neurons: excitatory cells that release the neurotransmitter glutamate and inhibitory interneurons that release the neurotransmitter GABA. Subsets of both types of cells are directly innervated by excitatory thalamic relay neurons, which are the main source of extrinsic input to the neocortex. Curiously, inhibitory interneurons respond much more strongly than excitatory cells to thalamic input[2–5]. These interneurons, in turn, synapse locally in the neocortex, producing robust feedforward inhibition in the same cells that receive direct thalamocortical excitation[6–11]. Although the consequences of feedforward inhibition have been extensively considered[12–14], little is known about the mechanisms of the strong interneuron activation that produces it. Obviously, understanding how both inhibitory and excitatory neurons in the neocortex respond to their principle external input is an essential step in understanding sensory information processing and perhaps other neocortex-dependent processes such as perception and cognition.

Here we demonstrate that the greater thalamocortical activation of inhibitory interneurons, compared with excitatory cells, is mediated by differences in their synaptic mechanisms, rather than their intrinsic membrane properties. The synaptic mechanisms include differences in the strength of direct thalamocortical excitation and the effectiveness of disynaptic feedforward inhibition. The latter is not due to a simple difference in inhibitory synaptic strength, but instead to dynamic properties of the cortical microcircuits, arising from cell type–specific differences in the relative kinetics of excitatory and inhibitory synaptic currents.

RESULTS

To test the mechanisms of thalamocortical responsiveness, we used an *in vitro* preparation, from mouse brain, that has intact connections between primary somatosensory thalamus and cortex (that is, ventrobasal thalamus (VB) and barrel cortex)[15]. We stimulated the VB with extracellular electrodes and recorded evoked responses simultaneously from pairs of layer 4 cells located in an aligned cortical barrel (Methods, **Fig. 1a**). Each pair consisted of one fast-spiking inhibitory interneuron (FS cell) and one regular-spiking excitatory neuron (RS cell), both of which received direct (monosynaptic) thalamic input (Methods and **Fig. 1** and **Supplementary Fig. 1** online)[3,8,10]. We chose closely spaced FS and RS cells (<50-μm separation) to ensure localization within common thalamocortical arbors. Initially, responses were recorded in a cell-attached configuration, so that the cell membrane and cytoplasm would remain intact. In pairs studied this way, thalamic stimuli usually evoked action potential responses in the FS cell (20/30 pairs), but rarely evoked action potentials in the RS cell (1/30 pairs), confirming and extending previous studies (**Fig. 1b**)[3,9,11].

In principle, the greater propensity of FS cells to spike in response to thalamic stimulation could have been due to differences in intrinsic membrane properties, synaptic mechanisms or both. In regard to intrinsic membrane properties, we hypothesized that FS cells would be more responsive if the difference between their resting potential and spike threshold was smaller than that of RS cells[16,17]. Whole-cell current clamp measurements showed, however, that the voltage differences between rest and threshold were not different for FS versus RS cells (**Fig. 1c,d**; $P = 0.182$, paired t-test; FS resting = –78.0 ± 0.8 mV, FS threshold = –48.8 ± 0.4 mV; RS resting = –79.3 ± 1.3 mV,

[1]Department of Neuroscience, Division of Biology & Medicine, Box G-LN, Brown University, Providence, Rhode Island 02912, USA. [2]Department of Mathematics, One Shields Avenue, University of California, Davis, Davis, California 95616, USA. Correspondence should be addressed to B.W.C. (barry_connors@brown.edu).

Received 20 October 2006; accepted 2 February 2007; published online 4 March 2007; doi:10.1038/nn1861

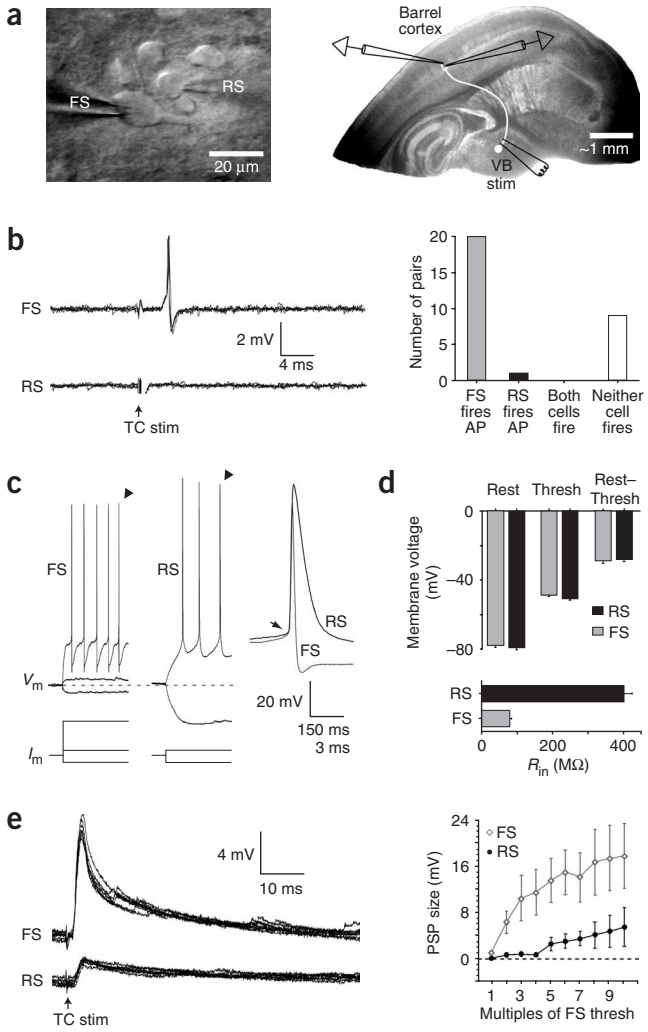

Figure 1 In paired FS-RS cell recordings, thalamocortical responses were strongest in FS cells, but intrinsic excitability was greatest in RS cells. (**a**) Left, differential interference contrast image of an FS-RS cell pair in layer 4 (pia toward left). Right, thalamocortical slice with schematic of experimental configuration (two patch electrodes in layer 4 barrel, stimulating electrode in VB). (**b**) Left, paired FS-RS cell recordings of thalamocortical (TC) responses in cell-attached mode (five sweeps; 128-μA stimulation; same cells as **a**). Action potentials can be observed ~3 ms after the thalamic stimulus in the FS cell. Right, tally of cell pairs exhibiting spike responses to VB stimuli (cell-attached; maximum stimulus = 256 μA; mean FS threshold =69 μA). Whole-cell recordings were made in 28 of the above pairs following cell-attached recordings to determine their thalamic input. All tested cells, RS and FS, received thalamic excitation. (**c**) Responses of FS-RS cell pair to injected current (I_{FS} = –60, +40, +280 pA; I_{RS} = –60, +40 pA; same pair as **a**,**b**). Voltage response to negative current step was smaller in FS than RS cell, reflecting lower R_{in}. Greater positive current was required to reach spike threshold in FS than RS cell (+280 pA versus +40 pA). Voltage thresholds for spiking were approximately equal (arrow, inset), as were resting potentials (baseline V_m). (**d**) Top, mean resting potentials (Rest), voltage thresholds for spikes (Thresh) and the differences between them (n = 17 pairs). Bottom, mean R_{in} (n = 17 pairs). (**e**) Left, thalamocortical PSPs were larger in FS than RS cells (paired whole-cell; seven sweeps; 120-μA VB stimulus = 2.4-fold greater PSP threshold; V_m = –79 mV). Right, mean thalamocortical PSPs. Stimulus intensities normalized to FS cell PSP thresholds (FS thresholds always ≤RS; n = 5 pairs). Error bars are s.e.m.

RS threshold = –51.1 ± 0.6 mV). Another intrinsic membrane property that can enhance excitability is a relatively high input resistance. However, we found that the input resistances of FS cells were about fivefold lower than those of RS cells ($P < 0.0001$; **Fig. 1c,d**; also see E.M. Goldberg and B. Rudy, *Soc. Neurosci. Abstr.* 736.732, 2005). Accordingly, FS cells required nearly sixfold more current than RS cells to reach spike threshold when directly depolarized via the recording electrodes (mean thresholds: FS = 304.3 ± 17.2 pA; RS = 51.5 ± 2.8 pA; **Fig. 1c**). Together, these data indicate that intrinsic membrane properties alone would actually make FS cells much less responsive than RS cells to thalamic input. This suggests that a synaptic basis for the cell-type differences in thalamocortical responsiveness is likely. Consistent with this, when thalamocortical postsynaptic potentials (PSPs) were evoked in FS-RS cell pairs, the PSPs were larger in FS than in RS cells across a wide range of stimulus intensities (**Fig. 1e**).

Three potential synaptic mechanisms might explain the FS-RS cell differences in thalamocortical responses: (i) excitatory input from the thalamus might be stronger in FS cells than in RS cells, (ii) feedforward inhibition onto FS cells could be weaker or (iii) differences in both excitation and inhibition could contribute. To test these possibilities, we measured synaptic currents evoked by thalamic stimuli in FS-RS cell pairs recorded in voltage clamp at varying holding potentials, and then calculated the associated excitatory and inhibitory conductances using conventional linear methods[18] (**Fig. 2a** and **Supplementary Methods** online).

The response of most FS cells to thalamocortical input began as a strong excitatory conductance (G_e), followed 1–3 ms later by an even stronger inhibitory conductance (G_i). This is illustrated for an example cell in **Figure 2a**. Thus, at depolarized holding potentials (between reversal potentials for excitation and inhibition), synaptic currents were biphasic: initially inward, then turning outward in a few milliseconds (**Fig. 2a**, I_{syn}). In comparison, the paired RS cell had weaker inward synaptic currents and a smaller peak G_e (**Fig. 2b**). The outward currents and peak G_i of the RS cell were also weaker than those of the FS cell.

We measured thalamically evoked G_e amplitudes in 15 FS-RS cell pairs using a variety of thalamic stimulus intensities (range: 2–8-fold greater than the PSC threshold). In nearly every case, the peak G_e was larger in the FS cell than in the simultaneously recorded RS cell (**Fig. 2c** $G_{exitatory}$). The average G_e of FS cells was 7.7-fold larger than that of RS cells (**Fig. 2c**; mean stimulus intensity was threefold greater than the PSC threshold). This G_e difference is undoubtedly an important factor for mediating the greater thalamocortical responsiveness of FS cells.

There are two possible explanations for the stronger excitatory conductances observed in FS cells: (i) greater numbers of thalamic VB cells might contact each FS cell and/or (ii) the unitary synaptic connections from VB to FS cells could be stronger than those from VB to RS cells. To estimate unitary strength, we used minimal stimulation of VB and simultaneously recorded the evoked EPSCs in FS-RS cell pairs (**Fig. 3**). The minimal stimulation approach[8,19] was applied in an attempt to activate the axons of single thalamic relay neurons projecting to the recorded cells (an example pair is shown in **Fig. 3b–e**). Stimuli just above threshold (29.7 μA in this case) evoked EPSCs in about half of the trials. Raising the stimulus intensity increased response probabilities without much effect on response amplitudes (up to 50 μA; **Fig. 3d**). In the example pair, the FS and RS cells had the same EPSC thresholds (**Fig. 3d,g**). Furthermore, the successful responses and failures occurred on common trials for the two cells (**Fig. 3d,e**); thus, it is likely that a single VB axon provided the threshold input to both cells[9,10,20]. Of the 20 pairs in which minimal responses were examined, 13 had equal EPSC thresholds for the FS and RS cells

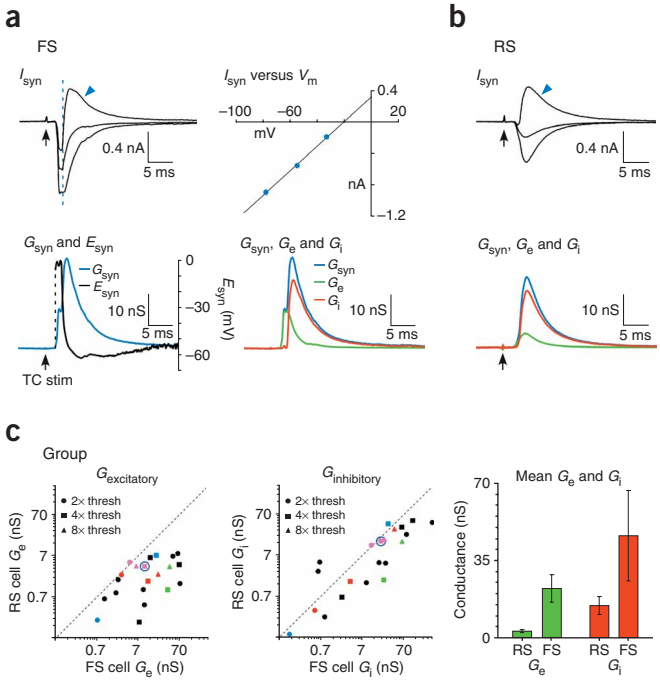

Figure 2 Excitatory and inhibitory conductances evoked by thalamocortical stimulation were larger in FS than in RS cells. (**a**) Synaptic currents and conductances for an FS cell. Upper left, TC-evoked synaptic currents (I_{syn}) recorded in FS cell, voltage clamped at three holding potentials (–35, –62, –88 mV; traces are means of ten sweeps; baseline currents subtracted). At –35 mV (blue arrowhead), the response was biphasic: inward-outward. Upper right, plot of synaptic current versus membrane potential (V_m) and linear regression at time of half-maximal conductance (indicated by dashed line in left panel). The slope and voltage intercept of regression line indicate synaptic conductance (G_{syn}) and reversal potential (E_{syn}). Lower left, continuous plots of G_{syn} and E_{syn} . Lower right, excitatory (G_e) and inhibitory (G_i) components of the total G_{syn}, calculated by comparing the measured E_{syn} to the assumed reversal potentials for excitation and inhibition (**Supplementary Methods**). (**b**) Responses of paired RS cell (conventions as **a**). Inward synaptic currents and G_e were smaller in RS than FS cell. (**c**) Group synaptic conductances. Left, G_e comparisons for all pairs (FS versus RS; peak amplitudes). Each data point shows responses for one pair at one stimulus intensity. Symbol shape indicates stimulus intensity (relative to PSC threshold). Symbol color differentiates cell pairs; for four pairs (red, green, blue and magenta), multiple intensities were tested. In 11 pairs, only one intensity was tested (black). G_e was larger in the FS than RS cell in 20/21 cases (points below diagonal). The circled point corresponds with the example in **a**,**b**. Middle, G_i amplitudes (conventions as for G_e). G_i was larger in FS than RS for the majority of pairs. Right, mean G_e and G_i ($n = 15$ pairs). Responses to multiple intensities were averaged, within cells, for contribution to group mean. G_e was larger in FS than RS cells ($P < 0.005$, paired t-test), whereas mean G_i values were not statistically different ($P = 0.095$). Error bars are s.e.m.

within a pair (**Fig. 3g**). Of these 13 pairs, 9 were similar to the example in that the FS and RS cells showed clear response failures and successes on matching trials (data not shown). Even when originating from a common presynaptic cell, the 'minimal EPSCs' usually had markedly different amplitudes in the two cortical neurons. As in the example, FS cells had the largest amplitudes in17 of 20 pairs (**Fig. 3c–f**), resulting in a 4.3-fold greater average (**Table 1**).

This cell type–specific difference in unitary strength is considerable, but it cannot fully account for the 7.7-fold difference in the 'compound' G_e amplitudes we observed previously with more intense stimulation (that is, at threefold greater than PSC threshold; **Fig. 2**). In fact, the sum of 7–8 average unitary VB inputs would be needed to equal the mean compound G_e size of FS cells, whereas only four would be required for RS cells (**Table 1**). Thus, individual FS cells apparently receive convergent input from more thalamic neurons than do individual RS cells. This conclusion is further supported by our observation that thalamocortical EPSC thresholds in FS cells were either lower than or equal to thresholds in RS cells, but never higher (**Fig. 3g**). Such a result can be best explained by the existence of higher effective densities of thalamic neurons projecting to FS than to RS cells[5], creating a closer mean proximity between the stimulating electrodes and FS-projecting thalamic neurons (thus the lower stimulus currents required for activation). In summary, the stronger compound thalamocortical G_e amplitudes observed in FS cells appear to result from both stronger unitary conductances and greater numbers of thalamic inputs per FS cell.

We also measured inhibitory conductances (G_i) evoked by the relatively intense thalamic stimuli (2–8-fold greater than PSC threshold). This feedforward inhibition is mainly produced disynaptically by the projections of local FS interneurons onto RS and other FS cells[2,8,9,11]. There are no known monosynaptic inhibitory projections from the VB to barrel cortex, and recurrent (that is, trisynaptic) inhibition would require strong RS cell spiking, which did not appear to occur here (**Fig. 1b**). Furthermore, the inhibitory conductance latencies were consistent with a disynaptic mechanism. Finally, most of the FS cells that fired action potentials in response to thalamic stimulation during cell-attached recordings (**Fig. 1b**) were subsequently found, during whole-cell recordings, to directly inhibit their paired RS cells (17/20 pairs, data not shown).

Inhibitory conductances tend to suppress responsiveness, so we reasoned that relatively large G_i values might contribute to the weak RS responses. However, we found that G_i amplitudes were larger in FS cells than in RS cells (17 of 21 paired comparisons; **Fig. 2c** $G_{inhibitory}$). The average G_i of FS cells was 3.2-fold greater than that of RS cells (**Fig. 2c**). Nevertheless, the functional inhibition produced in RS cells is likely to be stronger because the resting input conductances of FS cells are fivefold higher than those of RS cells (**Fig. 1c,d**, discussed below).

In addition to the amplitudes of thalamocortical synaptic conductances, we also examined whether the kinetics of these conductances might affect cell responsiveness. In general, excitatory conductances preceded inhibitory conductances by 1–2 ms, consistent with the monosynaptic nature of the thalamocortical projection versus the disynaptic nature of feedforward inhibition (**Fig. 4a–c**, and **Supplementary Fig. 2** online). Long delays between excitation and inhibition could allow for relatively full expression of excitatory responses before the onset of inhibition. We hypothesized that this might contribute to the stronger FS cell responses. To examine excitatory-inhibitory delays, we measured the latencies separating the G_e and G_i peaks. Consistent with our hypothesis, we found longer peak separations in FS than in RS cells (13 of 13 pairs; **Fig. 4a,b**). On average, peak separations were 2.0 ± 0.2 ms for FS, but only 0.5 ± 0.2 ms for RS cells. The difference was due to faster G_e kinetics in the FS cells (mainly faster rise times). Mean G_e onset latencies for FS cells and RS cells were 2.2 ± 0.1 and 2.6 ± 0.1 ms, and peak G_e latencies were 3.4 ± 0.1 and 4.8 ± 0.1 ms, respectively. In contrast, G_i kinetics were virtually identical for the two cell types; G_i peak latencies were 5.4 ± 0.2 and 5.3 ± 0.2 ms for FS cells and RS cells, respectively (**Fig. 4a–c**). The G_e responses were so fast in some FS cells that their peaks occurred before the onset of any substantial inhibition. In contrast, RS excitatory responses were often slow enough that inhibition was nearly maximal by the time of the G_e peak (**Fig. 4a**). To quantify this, we measured G_i amplitudes at the time of the G_e

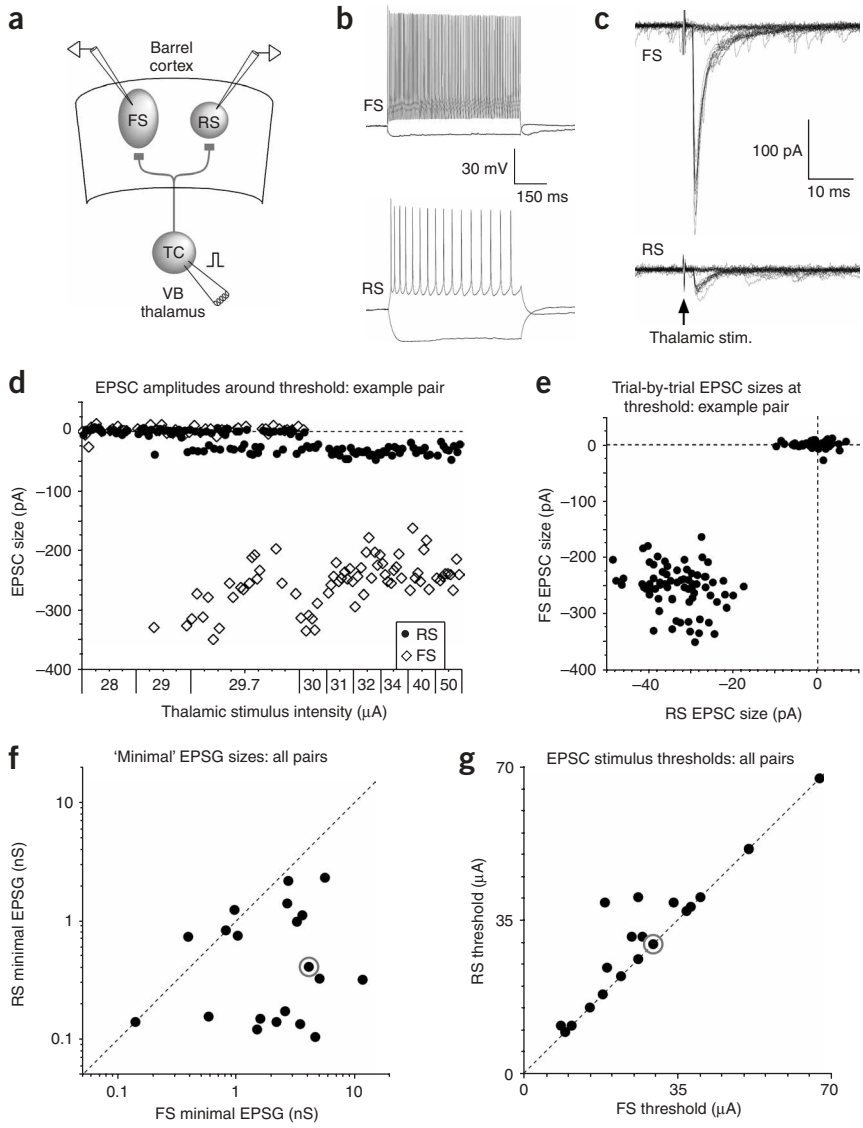

Figure 3 Strengths of individual thalamic cell connections, and the number of thalamic cells making connections, were greater for FS than for RS cells. (**a**) Schematic for testing unitary TC connections. (**b**–**e**) Data from an FS-RS cell pair. (**b**) Voltage responses to intracellular current steps showing typical FS and RS cell intrinsic properties ($I_{FS} = -100, +600$ pA; $I_{RS} = -100, +100$ pA). (**c**) Raw EPSCs (and failures) evoked by minimal VB stimulation (25 sweeps; 29.7-μA stimuli; –89-mV command). (**d**) EPSC amplitudes versus thalamic stimulus intensities. Raising stimulus intensities increased response probabilities without increasing amplitudes. (**e**) Data from **d**, replotted to compare FS and RS cell responses on individual trials. All trials with successful responses in one cell had successful responses in the other cell. (**f**) Synaptic conductances (EPSGs) evoked by minimal VB stimulation, across pairs ($n = 20$ pairs). EPSG calculations assumed a pure glutamatergic response with 0-mV reversal potential (EPSG = EPSC/$V_{holding}$). Seventeen of 20 pairs had larger EPSG in FS cell than in RS cell ($P < 0.002$, paired t-test). (**g**) EPSC stimulus thresholds across pairs ($n = 20$). In 13 of 20 pairs, FS and RS thresholds were equal. In 9 of these 13 pairs, the FS and RS cells either both responded or both failed to respond on any given trial, indicating innervation by the same thalamic axon (as in **e**). In the other 4 pairs with equal thresholds, response failures in one cell sometimes occurred during successes in the other, indicating that the minimal responses were mediated by different thalamic axons. In 7 of 20 pairs, the threshold was lower in the FS than the RS cell, again indicating different minimal inputs. The circled points in **f**,**g** correspond to the example pair from **b**–**e**.

peaks; we typically found larger values for the RS cells than for the FS cells (11 of 13 pairs; mean RS = 17.7 ± 4.8 nS, FS = 2.6 ± 0.8 nS; **Fig. 4d**). The high values on this G_i measure and the short G_i-G_e peak time separations both reflect a large degree of temporal overlap between thalamocortical excitation and feedforward inhibition in the RS cells. This overlap allows inhibition to effectively suppress excitatory responses, contributing to weaker RS cell responsiveness.

To determine the relative functional contributions of G_e-G_i kinetics versus amplitudes, we varied these factors independently in computational models of the FS and RS cells. The models were constructed using passive membrane properties and synaptic conductances derived directly from our experimental measurements (that is, the average values from the experiments; Methods, **Supplementary Fig. 2** and **Supplementary Methods**). When the FS and RS model cells were each injected with their default G_e waveforms (that is, the mean G_e waveforms recorded during the experiments shown in **Fig. 2**) in isolation, the resulting simulated EPSP was more than twice as large in the FS as in the RS cell (**Fig. 4e**, Default). By contrast, injection of the default G_i waveforms alone produced a slightly smaller IPSP in the FS than in the RS cell (**Fig. 4e**, Default), even though the FS cell's G_i amplitude was 3.2-fold larger in absolute terms (**Fig. 2c** and **Supplementary Fig. 2**). This discrepancy occurred mainly because the FS cell had a fivefold higher resting input conductance than the RS cell (**Fig. 1d** and **Supplementary Fig. 2**).

Notably, when the G_e and G_i waveforms were injected together (with the normal latencies and kinetics observed in the physiology experiments), the suppressive effect of inhibition on the resulting PSPs was much stronger in the RS than in the FS cell. Suppression of PSP amplitude in the RS cell was 83% (comparing the pure EPSP to the mixed PSP), whereas suppression in the FS cell was just 35% (**Fig. 4e**, Default). The greater RS cell suppression was due partly to greater functional inhibitory strength (that is, a higher ratio of G_i to total conductance) and partly to greater temporal overlap between G_e and G_i. To assess the relative effect of temporal overlap, we swapped synaptic conductance waveform kinetics (latencies and shapes) between the two model cells while

Table 1 Compound versus unitary excitatory thalamocortical conductances

	Compound G_e	Unitary G_e	Compound/unitary
FS cells	22.4 nS (± 6.1)	3.0 nS (± 0.6)	22.4/3.0 = 7.5
RS cells	2.9 nS (± 0.6)	0.7 nS (± 0.2)	2.9/0.7 = 4.1

Data are means ± s.e.m. of the peak excitatory conductances. Compound responses evoked by VB stimuli averaging threefold greater than the PSC threshold ($n = 15$ pairs). Unitary responses evoked by minimal VB stimuli (~PSC threshold) ($n = 20$ pairs).

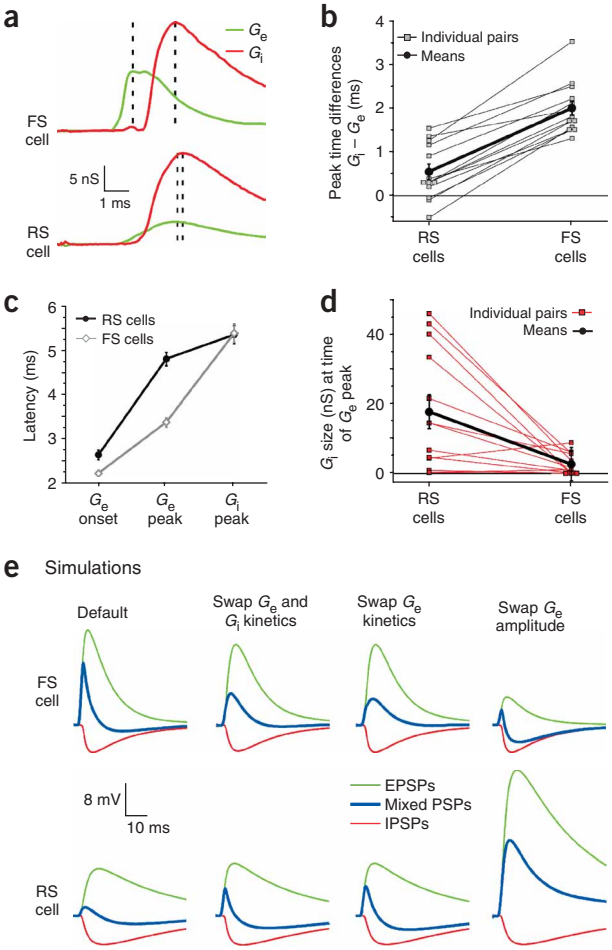

Figure 4 A cell-type difference in G_e-G_i kinetics allowed inhibition to be most effective in RS cells. (**a**) G_e and G_i from an example pair (same as **Fig. 2**). In the FS cell, G_e peaked 1.65 ms before G_i (dashed lines). In the RS cell, the peaks were only 0.25 ms apart. (**b**) G_i-G_e peak separation, across cells. Thin lines connect cells within pairs. Thick line connects group means. All pairs had greatest separation in the FS cell (13/13; $P < 0.0001$, paired *t*-test). (**c**) Mean latencies, referenced to thalamic stimulus. G_e latencies were shorter for FS than RS cells ($P < 0.002$, paired *t*-tests), but G_i latencies were nearly identical ($P = 0.885$). (**d**) Amplitude of G_i at time of G_e peak was largest for the RS cell in 11 of 13 pairs ($P < 0.01$, paired *t*-test). Error bars are s.e.m. (**e**) Modeling results. Left, simulated postsynaptic potentials to injection of default conductance waveforms (green, G_e alone; red, G_i alone; blue, G_e and G_i). Middle left, G_e and G_i conductance kinetics were swapped between cells while holding amplitudes constant (see **Supplementary Methods**). This decreased the mixed PSP in the FS cell and increased it in the RS. Middle right, G_e kinetics alone were swapped, producing effects similar to those when both G_e and G_i kinetics were swapped. Right, G_e amplitudes were swapped between cells while kinetics were held constant. This also decreased the mixed PSP in the FS cell and increased it in the RS cell.

holding amplitudes at default levels (see **Supplementary Methods**). This greatly decreased inhibitory suppression in the RS cell and increased suppression in the FS; the mixed PSPs were now suppressed 48% (RS cell) and 61% (FS cell) relative to their respective pure EPSPs (**Fig. 4e**, Swap G_e and G_i kinetics). Swapping G_e kinetics alone had nearly the same effect as swapping both G_e and G_i kinetics (**Fig. 4e**, Swap G_e kinetics) because G_i kinetics were quite similar between RS and FS cells (**Fig. 4a–c** and **Supplementary Fig. 2**).

These simulation results indicate that a substantial fraction (approximately 75%) of the cell-type difference in inhibitory suppression was due to differences in G_e-G_i overlap, resulting mostly from differences in G_e kinetics. Moreover, swapping the G_e kinetics between cell types more than tripled the RS cell's mixed PSP size and decreased the FS cell's mixed PSP size by 58% (**Fig. 4e**, Default versus Swap G_e kinetics). Thus, on the basis of the results from these simple models it appears that kinetic differences can have powerful effects on the PSPs. The kinetic effects also seem to make the two cell types differentially sensitive to inhibitory driving force—that is, to the voltage difference between the inhibitory reversal potential and the ongoing membrane potential. Our modeling studies indicate that thalamocortical PSP responses in RS cells are greatly affected by inhibitory driving force, being strongly suppressed if there is hyperpolarizing inhibition, but only weakly suppressed if there is shunting inhibition (when the inhibitory reversal potential is near the resting potential; **Supplementary Fig. 3** online). In contrast, thalamocortical feedforward inhibition in FS cells appears to be quite ineffective even when there is a relatively strong hyperpolarizing driving force. This is because the thalamocortical excitatory conductances produced in FS cells are very fast, peaking before the inhibitory conductances become significant (**Supplementary Fig. 3**). Inhibitory driving force can vary widely across experimental conditions[21–25], or even within experiments *in vivo*, as membrane potentials fluctuate with cortical state[26,27]. Thus, the effects described here may point to a mechanism by which state could differentially regulate the sensory responses of FS and RS cells.

Finally, we attempted to assess the relative contribution of the cell type–specific differences in G_e amplitudes. We swapped G_e amplitudes between the two model cells, while holding other conductance features (G_e kinetics; G_i amplitudes and kinetics) at default levels. The resulting PSPs increased more than ninefold in the RS cell and decreased 76% in the FS cell (**Fig. 4e**, Default versus Swap G_e amplitude). On the basis of these measures, it appears that the cell type–specific differences in G_e amplitudes have an even greater influence than synaptic kinetics on PSP response sizes (more than twofold).

DISCUSSION

A major finding of this study is that the stronger thalamocortical responses of FS inhibitory interneurons, compared with excitatory neurons, are due to synaptic mechanisms, with no apparent positive contribution by intrinsic membrane properties. This differs from the situation in the hippocampus, where depolarized resting potentials tend to make interneurons more intrinsically responsive than neighboring excitatory neurons (reviewed in ref. 17). We found virtually no cell type–specific differences in membrane potential or spike threshold in neocortical FS and RS cells. Furthermore, the very low input resistances of FS interneurons tended to decrease, rather than increase, their excitability. The FS cells did have faster membrane time constants than RS cells (mean FS versus RS: 9.0 ± 0.5 versus 27.9 ± 1.3 ms). However, because these fast time constants were produced by low R_{in} rather than capacitance (mean input capacitance was higher in FS cells than in RS: 114.1 ± 5.6 versus 71.4 ± 3.0 pF), the net effect would tend to slow the absolute rates of the rise of FS cell PSPs (**Supplementary Fig. 4** online). Although the incidence of thalamic stimulus-evoked spiking observed here is consistent with previous *in vitro* studies (for example, ref. 3), it is rather low compared with expectations from *in vivo* studies of sensory-evoked spiking[28]. This difference may have several causes, including (i) fewer intact thalamocortical axons in slices than *in vivo*, (ii) failure to activate the full complement of thalamocortical neurons projecting to the cortical cells, (iii) relatively hyperpolarized resting potentials in the slices or (iv) effects of

neuromodulators whose levels may be depressed in slices. It will be important to reconcile these differences in future studies.

One synaptic mechanism contributing to the greater responses in FS cells was their stronger excitatory conductances. On average, G_e amplitudes in FS cells were 7.7-fold greater than in RS cells. This finding is compatible with previous *in vitro* studies showing that FS cells generally have stronger thalamocortical inward currents or EPSPs[2,3,8,9,11]. The larger EPSPs are very likely to contribute to the stronger evoked spiking in FS cells[29]. In paired FS-RS cell recordings, we found that excitatory conductances themselves were almost always larger in FS cells. Furthermore, we found that the mechanisms for inducing the larger compound excitatory conductances in FS cells included larger unitary thalamocortical conductances[9] and innervation by greater numbers of thalamic cells. Both of these characteristics are consistent with extracellular *in vivo* findings[4,5]. However, the innervation difference conflicts with a recent *in vitro* study indicating that equal numbers of VB neurons innervate FS and RS cells[9]; this requires further attention. Future studies should also determine how the relative strengths of thalamocortical conductances in FS versus RS cells change during physiologically realistic repetitive patterns of stimulation. For example, it has previously been shown that short-term synaptic depression of thalamocortical EPSPs is more pronounced in FS than in RS cells[8]. This could contribute to a greater depression of feedforward inhibition compared with monosynaptic excitation during repeated stimulation[9] (but see ref. 28).

Another synaptic mechanism contributing to the stronger FS responses was the cell type–specific difference in G_e-G_i kinetics. The excitatory conductances of FS cells rose quickly, allowing for action potentials before the onset of significant inhibition. In contrast, the excitatory conductances of RS cells were slow to rise, and therefore were suppressed by overlapping inhibition. In the neocortex[30–32] and hippocampus[33,34], interneurons generally express AMPA receptors with very fast EPSC kinetics that often lack the GluR2 subunit (reviewed in refs. 16,17). These specialized receptors are likely to contribute to the faster thalamocortical excitation of FS cells observed here. Another factor that could have apparent effects on G_e kinetics is the electrotonic position of the synapses[34]. In fact, there is clear evidence that thalamocortical terminals tend to innervate the somata of interneurons more densely than the somata of excitatory neurons[20,35–38]; this is consistent with faster synaptic responses. However, the majority of thalamocortical synapses exist on dendrites, even in inhibitory cells[20,36,38], so a more meaningful comparison would involve thalamocortical synapse density as a function of dendritic position for inhibitory versus excitatory cells. To our knowledge, no conclusive studies of this kind exist.

The kinetic effects we observed are reminiscent of recent *in vivo* findings of a study examining sensory responses of RS cells in barrel cortex[39]. Optimally oriented whisker stimuli, which elicited robust spike responses, produced G_e-G_i sequences with maximal temporal separation[39]. These findings suggest that G_e-G_i timing is a cellular mechanism of sensory coding[40], permitting spike responses to preferred stimuli and suppressing spikes to other stimuli. If so, then FS cells, which have broad suprathreshold receptive fields[4,5], would be predicted to have robust separation between G_e and G_i for equally broad ranges of sensory stimuli. This prediction is supported by our *in vitro* findings. Across experiments, the electrical stimuli presumably activated thalamocortical afferents with many different stimulus preferences, and activation of those varied afferents consistently elicited responses with strong G_e-G_i separation in FS cells.

Decades of research have shown that sensory stimulation yields thalamocortical excitation in the neocortex that is yoked with exquisite temporal precision to strong feedforward inhibition. Our results reveal the synaptic mechanisms by which this feedforward inhibition is initiated.

METHODS

All procedures were approved by the Brown University Institutional Animal Care and Use Committee. Somatosensory thalamocortical slices (375–425 μm thick, 35° tilt from coronal plane) were obtained from mice aged postnatal day 13–18 as previously described[8,15]. Mice were either standard outbred strains (ICR, Swiss Webster) or F1 hybrids created by crossing ICR mice with the transgenic line G42. The G42 mice express enhanced green fluorescent protein (GFP) in a subset of parvalbumin-expressing GABAergic interneurons, under the control of a GAD67 gene promoter[41]. The GFP-expressing cells in this line have FS physiological characteristics (**Supplementary Fig. 1**, below). Experiments were conducted at 32 °C in a submersion-style recording chamber. The slices were bathed in artificial cerebrospinal fluid (ACSF) containing 126 mM NaCl, 3 mM KCl, 1.25 mM NaH_2PO_4, 2 mM $MgSO_4$, 26 mM $NaHCO_3$, 10 mM dextrose and 2 mM $CaCl_2$, then saturated with 95% O_2/5% CO_2. For whole-cell current clamp recordings, patch pipettes were filled with 130 mM potassium gluconate, 4 mM KCl, 2 mM NaCl, 10 mM HEPES, 0.2 mM EGTA, 4 mM ATP-Mg, 0.3 mM GTP-Tris and 14 mM phosphocreatine-Tris (pH 7.25, ~290 mOsm). For voltage clamp recordings, cesium was substituted for potassium in the patch pipettes to reduce potassium conductances, and 50 μM APV was added to the bathing solution to remove nonlinearities in the synaptic conductances associated with NMDA receptors. Experiments were conducted using Axon Instruments hardware and software (Axoclamp 2B, Digidata 1322A, pClamp 9). Series resistances (usually 10–20 MΩ) were monitored throughout the experiments; they were compensated on-line in current clamp recordings and off-line for voltage clamp recordings (**Supplementary Methods**)[18]. Membrane potentials were corrected for a 14-mV liquid junction potential. Statistical P values were calculated using paired t-tests. Error bars in figures are s.e.m.

To activate thalamic afferents, extracellular stimuli were delivered to the VB through paired microwires (FHC: 25-μm diameter bipolar, 4–256 μA, 0.2-ms pulses; either single pulses or trains of 3–4 pulses were presented at 10-s intervals, and intratrain frequency was 20 Hz). The cortex was initially mapped with extracellular recordings to find the barrel that was best aligned with the VB stimulation site (that is, the barrel with the largest VB-evoked field potential). Paired FS-RS recordings were then made in the aligned layer 4 barrel (**Fig. 1a**). Cells were visualized with infrared differential interference contrast and fluorescence microscopy. Initial targeting was mainly by size (RS cells are relatively small, FS cells are large), but the presence of a single, prominent descending dendrite emerging from a large tapered soma was also indicative of layer 4 FS cells (**Fig. 1a**). In G42 mice, GFP expression was used to target FS cells (above, **Supplementary Fig. 1**). After patching onto the neurons, thalamocortical-evoked spikes were recorded in cell-attached mode (**Fig. 1b**). Subsequently, membranes were ruptured to achieve whole-cell configurations, and then neurons were identified by intrinsic membrane characteristics as previously described[8]. Only FS and RS cells were used here; other cell types such as low-threshold spiking cells were not analyzed[8]. Resting potentials were measured within 2 min of break-in, and then steady-state potentials were usually adjusted to –79 mV (the mean resting potential) with intracellular current. Membrane time constants (τ_m), input resistances (R_{in}) and input capacitances (C_{in}) were calculated from voltage responses to small negative current pulses (typically –50 pA, 600 ms). For τ_m, the voltage responses were fitted with single exponentials, skipping the initial 3 ms, and ending before any voltage 'sag' became apparent. R_{in} was determined from Ohm's law. C_{in} was calculated as τ_m / R_{in}. Intrinsic spiking properties were characterized with 600-ms positive current steps. The current threshold was defined as the lowest amplitude step that elicited spikes (20–50 pA step size). Voltage threshold was the membrane potential at the point of greatest change in the slope of the membrane potential determined by visual inspection. Spike width was measured at half amplitude. After-hyperpolarization was measured as the voltage change from spike threshold to the trough following the spike. Compared with RS cells, FS cells had narrow spikes (FS range = 0.25–0.41 ms; RS range = 0.72–1.07 ms), large fast after-hyperpolarizations and high maximal firing rates

with very little frequency adaptation (**Fig. 1c** and **3b**)[8]. Other differences in intrinsic characteristics are addressed in the main text.

Thalamocortical synaptic conductances were determined from slopes of synaptic current-voltage relationships (**Fig. 2a**). The excitatory and inhibitory contributions to thalamocortical conductances were calculated by comparing the measured reversal potential of the total synaptic conductance with the assumed reversal potentials for excitation and inhibition (**Supplementary Methods** and **Fig. 2a**)[18].

Simulations of thalamocortical responses were performed in single-compartment models of FS and RS cells. The inhibitory and excitatory synaptic conductance waveforms, as well as the passive intrinsic membrane properties (τ_m, R_{in} and C_{in}), were set to the average values recorded during the physiology experiments. No voltage-dependent intrinsic conductances were included. See **Supplementary Methods** for details (**Fig. 4e** and **Supplementary Fig. 2**).

Note: Supplementary information is available on the Nature Neuroscience website.

ACKNOWLEDGMENTS

We thank our colleagues A. Agmon, O. Ahmed, C. Aizenman, J.-M. Edeline, E. Fanselow, A. Gray, S.-C. Lee, M. Long, R. Metherate, K. Pratt, K. Richardson, B. Rudy and H. Swadlow for their helpful comments about this work; S. Patrick for technical assistance; and Z. Huang for providing G42 mice. Our research was supported by grants from the US National Institutes of Health, the US National Science Foundation and the Brown University Brain Science Program.

COMPETING INTERESTS STATEMENT

The authors declare no competing financial interests.

Published online at http://www.nature.com/natureneuroscience
Reprints and permissions information is available online at http://npg.nature.com/reprintsandpermissions

1. Mountcastle, V.M. *Perceptual Neuroscience* (Harvard University Press, Cambridge, Massachusetts, USA, 1998).
2. Gibson, J.R., Beierlein, M. & Connors, B.W. Two networks of electrically coupled inhibitory neurons in neocortex. *Nature* **402**, 75–79 (1999).
3. Porter, J.T., Johnson, C.K. & Agmon, A. Diverse types of interneurons generate thalamus-evoked feedforward inhibition in the mouse barrel cortex. *J. Neurosci.* **21**, 2699–2710 (2001).
4. Bruno, R.M. & Simons, D.J. Feedforward mechanisms of excitatory and inhibitory cortical receptive fields. *J. Neurosci.* **22**, 10966–10975 (2002).
5. Swadlow, H.A. Thalamocortical control of feedforward inhibition in awake somatosensory 'barrel' cortex. *Phil. Trans. R. Soc. Lond. B* **357**, 1717–1727 (2002).
6. Agmon, A. & Connors, B.W. Correlation between intrinsic firing patterns and thalamocortical synaptic responses of neurons in mouse barrel cortex. *J. Neurosci.* **12**, 319–329 (1992).
7. Gil, Z. & Amitai, Y. Properties of convergent thalamocortical and intracortical synaptic potentials in single neurons of neocortex. *J. Neurosci.* **16**, 6567–6578 (1996).
8. Beierlein, M., Gibson, J.R. & Connors, B.W. Two dynamically distinct inhibitory networks in layer 4 of the neocortex. *J. Neurophysiol.* **90**, 2987–3000 (2003).
9. Gabernet, L., Jadhav, S.P., Feldman, D.E., Carandini, M. & Scanziani, M. Somatosensory integration controlled by dynamic thalamocortical feedforward inhibition. *Neuron* **48**, 315–327 (2005).
10. Inoue, T. & Imoto, K. Feedforward inhibitory connections from multiple thalamic cells to multiple regular-spiking cells in layer 4 of the somatosensory cortex. *J. Neurophysiol.* **96**, 1746–1754 (2006).
11. Sun, Q.Q., Huguenard, J.R. & Prince, D.A. Barrel cortex microcircuits: thalamocortical feedforward inhibition in spiny stellate cells is mediated by a small number of fast-spiking interneurons. *J. Neurosci.* **26**, 1219–1230 (2006).
12. Miller, K.D., Pinto, D.J. & Simons, D.J. Processing in layer 4 of the neocortical circuit: new insights from visual and somatosensory cortex. *Curr. Opin. Neurobiol.* **11**, 488–497 (2001).
13. Douglas, R.J. & Martin, K.A. Neuronal circuits of the neocortex. *Annu. Rev. Neurosci.* **27**, 419–451 (2004).
14. Alonso, J.M. & Swadlow, H.A. Thalamocortical specificity and the synthesis of sensory cortical receptive fields. *J. Neurophysiol.* **94**, 26–32 (2005).
15. Agmon, A. & Connors, B.W. Thalamocortical responses of mouse somatosensory (barrel) cortex *in vitro*. *Neuroscience* **41**, 365–379 (1991).
16. Lawrence, J.J. & McBain, C.J. Interneuron diversity series: containing the detonation-feedforward inhibition in the CA3 hippocampus. *Trends Neurosci.* **26**, 631–640 (2003).
17. Jonas, P., Bischofberger, J., Fricker, D. & Miles, R. Interneuron diversity series: fast in, fast out—temporal and spatial signal processing in hippocampal interneurons. *Trends Neurosci.* **27**, 30–40 (2004).
18. Wehr, M. & Zador, A.M. Balanced inhibition underlies tuning and sharpens spike timing in auditory cortex. *Nature* **426**, 442–446 (2003).
19. McNaughton, B.L., Barnes, C.A. & Andersen, P. Synaptic efficacy and EPSP summation in granule cells of rat fascia dentata studied in vitro. *J. Neurophysiol.* **46**, 952–966 (1981).
20. Staiger, J.F., Zilles, K. & Freund, T.F. Distribution of GABAergic elements postsynaptic to ventroposteromedial thalamic projections in layer IV of rat barrel cortex. *Eur. J. Neurosci.* **8**, 2273–2285 (1996).
21. Martina, M., Royer, S. & Pare, D. Cell type–specific GABA responses and chloride homeostasis in the cortex and amygdala. *J. Neurophysiol.* **86**, 2887–2895 (2001).
22. Owens, D.F. & Kriegstein, A.R. Is there more to GABA than synaptic inhibition? *Nat. Rev. Neurosci.* **3**, 715–727 (2002).
23. Gulledge, A.T. & Stuart, G.J. Excitatory actions of GABA in the cortex. *Neuron* **37**, 299–309 (2003).
24. Jin, X., Huguenard, J.R. & Prince, D.A. Impaired Cl^- extrusion in layer V pyramidal neurons of chronically injured epileptogenic neocortex. *J. Neurophysiol.* **93**, 2117–2126 (2005).
25. Szabadics, J. *et al.* Excitatory effect of GABAergic axo-axonic cells in cortical microcircuits. *Science* **311**, 233–235 (2006).
26. Steriade, M., Timofeev, I. & Grenier, F. Natural waking and sleep states: a view from inside neocortical neurons. *J. Neurophysiol.* **85**, 1969–1985 (2001).
27. Bruno, R.M. & Sakmann, B. Cortex is driven by weak but synchronously active thalamocortical synapses. *Science* **312**, 1622–1627 (2006).
28. Higley, M.J. & Contreras, D. Balanced excitation and inhibition determine spike timing during frequency adaptation. *J. Neurosci.* **26**, 448–457 (2006).
29. Galarreta, M. & Hestrin, S. Spike transmission and synchrony detection in networks of GABAergic interneurons. *Science* **292**, 2295–2299 (2001).
30. Geiger, J.R. *et al.* Relative abundance of subunit mRNAs determines gating and Ca^{2+} permeability of AMPA receptors in principal neurons and interneurons in rat CNS. *Neuron* **15**, 193–204 (1995).
31. Lambolez, B., Ropert, N., Perrais, D., Rossier, J. & Hestrin, S. Correlation between kinetics and RNA splicing of α-amino-3-hydroxy-5-methylisoxazole-4-propionic acid receptors in neocortical neurons. *Proc. Natl. Acad. Sci. USA* **93**, 1797–1802 (1996).
32. Zhou, F.M. & Hablitz, J.J. AMPA receptor–mediated EPSCs in rat neocortical layer II/III interneurons have rapid kinetics. *Brain Res.* **780**, 166–169 (1998).
33. Geiger, J.R., Lubke, J., Roth, A., Frotscher, M. & Jonas, P. Submillisecond AMPA receptor–mediated signaling at a principal neuron-interneuron synapse. *Neuron* **18**, 1009–1023 (1997).
34. Walker, H.C., Lawrence, J.J. & McBain, C.J. Activation of kinetically distinct synaptic conductances on inhibitory interneurons by electrotonically overlapping afferents. *Neuron* **35**, 161–171 (2002).
35. Benshalom, G. & White, E.L. Quantification of thalamocortical synapses with spiny stellate neurons in layer IV of mouse somatosensory cortex. *J. Comp. Neurol.* **253**, 303–314 (1986).
36. Keller, A. & White, E.L. Synaptic organization of GABAergic neurons in the mouse SmI cortex. *J. Comp. Neurol.* **262**, 1–12 (1987).
37. Ahmed, B., Anderson, J.C., Douglas, R.J., Martin, K.A. & Nelson, J.C. Polyneuronal innervation of spiny stellate neurons in cat visual cortex. *J. Comp. Neurol.* **341**, 39–49 (1994).
38. Ahmed, B., Anderson, J.C., Martin, K.A. & Nelson, J.C. Map of the synapses onto layer 4 basket cells of the primary visual cortex of the cat. *J. Comp. Neurol.* **380**, 230–242 (1997).
39. Wilent, W.B. & Contreras, D. Dynamics of excitation and inhibition underlying stimulus selectivity in rat somatosensory cortex. *Nat. Neurosci.* **8**, 1364–1370 (2005).
40. Moore, C.I., Nelson, S.B. & Sur, M. Dynamics of neuronal processing in rat somatosensory cortex. *Trends Neurosci.* **22**, 513–520 (1999).
41. Chattopadhyaya, B. *et al.* Experience and activity-dependent maturation of perisomatic GABAergic innervation in primary visual cortex during a postnatal critical period. *J. Neurosci.* **24**, 9598–9611 (2004).